Branching ratios for $\bar{p}p$ annihilation at rest into two-body final states

Crystal Barrel Collaboration

This draft written by

C.J. Batty [b], E. Klempt [a], B. Pick [a],

[a] *Universität Bonn, D-53115 Bonn, FRG*

[b] *Rutherford Appleton Laboratory, Chilton, Didcot OX11 0QX, UK*

Abstract

Measurements of two-body branching ratios for $\bar{p}p$ annihilations at rest in liquid and gaseous ($12\,\rho_{STP}$) hydrogen are reported. Channels studied are $\bar{p}p \to \pi^0\pi^0$, $\pi^0\eta$, $K^0_L K^0_S$, $\pi^+\pi^-$ and K^+K^-. The results are critically compared with those from other experiments. Values of the fraction of P-state annihilation for a range of target densities from $0.002\,\rho_{STP}$ to liquid H_2 are determined.

1 Introduction

In a previous paper [1] we have reported a measurement of the branching ratio $BR(\pi^0\pi^0, liq)$ for the annihilation reaction $\bar{p}p \to \pi^0\pi^0$ at rest in liquid hydrogen. Further details about this measurement and results for a wide range of other two-body channels are given in [2]. As pointed out in [1] our measured branching ratio for the $\pi^0\pi^0$ channel, with detection of all 4 photons, is significantly larger than previously measured values where only 2 or 3 photons from the decay of the 2 pions were detected. When combined with the branching ratio measurement for $\bar{p}p \to \pi^+\pi^-$ from 2P-states [3], it gave an unexpectedly large value for the fraction of P-state annihilation in liquid hydrogen. However it was also pointed out in [1] that a much smaller P-state fraction would be obtained when the differing strong interaction widths of the fine structure levels [4] are taken into account. These ideas were placed on a more quantitative basis by Batty [5] and a P-state fraction of 0.13 ± 0.04 in liquid hydrogen was obtained from an analysis of a wide range of branching ratio measurements. This P-state fraction is in accord with the expectations of cascade calculations including Stark mixing effects [5,6].

Recently the Obelix collaboration, in a measurement where also all 4 photons were detected, obtained [7] the value $BR(\pi^0\pi^0, liq) = (2.8 \pm 0.4)10^{-4}$ which is again much lower than the Crystal Barrel value [1,2] of $BR(\pi^0\pi^0, liq) = (6.93 \pm 0.43)10^{-4}$. The aim of the present paper is to measure this and other two-body branching ratios by a re-analysis of the old Crystal Barrel data, a new analysis of recent data and to extend the measurements to annihilation in gaseous hydrogen at $12\,\rho_{\mathrm{STP}}$, where ρ_{STP} is the density of H_2 gas at STP. These latter measurements enable the fraction of P-state annihilation to be studied as a function of H_2 target density [5,6].

2 Apparatus

The measurements were carried out using the Crystal Barrel detector at LEAR. A detailed description of the apparatus, as used for early data taking (1989 onwards), has been given elsewhere [8]. To study annihilation at rest, a beam of 200 MeV/c antiprotons extracted from LEAR, stopped in a liquid hydrogen target at the center of the detector. The whole detector was situated in a 1.5 T solenoidal magnet with the incident antiproton beam direction along its axis. The target was surrounded by a pair of multiwire proportional chambers (PWC's) and a cylindrical jet drift chamber (JDC) with 30 sectors, each sector having 23 sense wires at radial distances between 63 mm and 239 mm. The JDC was surrounded by a barrel shaped calorimeter consisting of 1380 CsI(Tl) crystals in a pointing geometry. The CsI calorimeter covered the polar angles between 12° and 168° with full coverage in azimuth. The overall acceptance for shower detection was $0.95 \times 4\pi$ sr. Typical photon energy resolutions were $\sigma_E/E = 2.5\%$ at 1 GeV, and $\sigma_{\phi,\vartheta} = 1.2°$ in both polar and azimuthal angles. The mass resolution was $\sigma = 10$ MeV for π^0 and 17 MeV for $\eta \to 2\gamma$.

In 1995 the PWC's were replaced by a microstrip vertex detector (SVTX) consisting of 15 single-sided silicon detectors, each having 128 strips with a pitch of 50 μm running parallel to the beam axis [9]. As well as giving improved identification of secondary vertices, this detector provided better vertex resolution in r, ϕ and improved momentum determination with a resolution $\Delta p/p$ for charged tracks of 3.4% at 0.8 GeV/c and 4.2% at 1.0 GeV/c. To study annihilation in hydrogen gas, the liquid target was replaced by a Mylar vessel with 230 μm thick walls and a 195 μm thick entrance window, containing hydrogen gas at room temperature and 12 bar pressure. A 55 μm thick Si detector was used to count the incident 100 MeV/c antiproton beam.

3 Experimental

3.1 Minimum bias data

An important feature of the present paper is a new analysis of recent Crystal Barrel data which avoids possible biases due to kinematic fitting. The data were selected solely on the basis of an $\mid \vec{p_{\rm tot}} \mid$ vs $E_{\rm tot}$ plot of 4γ events and the invariant mass of $\gamma\gamma$ combinations. Here $E_{\rm tot}$ is the total energy of the event and $\mid \vec{p_{\rm tot}} \mid$ the total momentum. The analysis of the data taken with a liquid H_2 target will first be described in some detail.

The data were taken in April 1996 and comprise 1 801 267 events taken with a minimum bias trigger on incident antiprotons entering the liquid H_2 target. After excluding events with the pile-up flag set, where a second antiproton entered the target within the time range from 7 μs before to 4 μs after the trigger antiproton, 1 591 407 events remained. Of these events 1 312 753 contained charged tracks which when reconstructed gave a z-distribution along the beam direction with two peaks; a large peak at the target centre and a smaller one at $z = -3.1$ cm corresponding to antiprotons annihilating in the Si beam counter and target entrance region. A fit gave $(3.7 \pm 0.7)\%$ of events corresponding to antiprotons not stopping in the hydrogen target. Since no kinematic fit is applied in the data selection, the final two-body events include in-flight annihilation as does the reference data set of minimum bias events. The in-flight contribution amounts to about 6% [2]. Assuming the branching ratio does not change for annihilation at very low momentum, the effect cancels out in the two data sets and no correction was therefore applied for in-flight annihilations.

Of the 278 654 events with no charged track, events with photons hitting the crystal rings adjacent to the entrance/exit holes were rejected since part of the energy may have escaped detection. Clusters of energy with the central crystal having an energy < 13 MeV were also not used since they originate mainly from shower fluctuations and not from primary photons. From the events remaining after the preselection, the 4γ events were selected and the momenta and invariant masses of all six $\gamma\gamma$ combinations calculated (See Fig. 1). Each $\pi^0\pi^0$ event gives two entries in the peak on the right hand side of the momentum plot (Fig. 1(a)) A large peak for π^0 and a smaller one for η events are visible in the plot of invariant masses (Fig. 1(b)) To suppress background due to wrong $\gamma\gamma$ combinations and from other annihilation channels, then from all six $\gamma\gamma$ combinations the one with the smallest distance d to the masses of the desired particles m_a and m_b was chosen.

$$d = \mid m_i(\gamma\gamma) - m_a \mid + \mid m_j(\gamma\gamma) - m_b \mid \qquad (1)$$

provided that for each of the two terms on the right hand side

$$\mid m_{i,j}(\gamma\gamma) - m_{a,b} \mid < 50\,\mathrm{MeV} \tag{2}$$

A plot of the measured total momentum $\mid \vec{p_{\mathrm{tot}}} \mid$ as a function of the total energy E_{tot} is shown in figure 2. The expected clustering of events at $E = 2m_{\mathrm{p}}c^2 = 1877\,\mathrm{MeV}$ and $\mid \vec{p_{\mathrm{tot}}} \mid = 0$ is clearly seen together with a further grouping around $E = 2m_{\mathrm{p}}c^2 - m_{\mathrm{K_L}}c^2 = 1379\,\mathrm{MeV}$ and $\mid \vec{p_{\mathrm{tot}}} \mid = 795\,\mathrm{MeV}/c$ corresponding to $\bar{\mathrm{p}}\mathrm{p} \rightarrow \mathrm{K^0_S K^0_L}$ events with $\mathrm{K^0_S} \rightarrow \pi^0\pi^0$ and an undetected (i.e. non-interacting) $\mathrm{K^0_L}$. Also shown are the kinematic regions used to select the desired two-body events. The selected region used to give the final value of the branching ratio was chosen to be small enough so as to reduce any contribution from background events, but large enough so that the desired events were not rejected and the detection efficiency, as determined by Monte Carlo simulation, was not reduced. In practice it proved straightforward to choose a suitable region which both satisfied the above conditions and also gave branching ratios which were insensitive, within the experimental statistical errors, to reasonable changes in the limits chosen for $\mid \vec{p_{\mathrm{tot}}} \mid$ and E_{tot}.

Figure 3(a) shows the momentum of $\gamma\gamma$ pairs for the $\pi^0\pi^0$ final state which satisfy equs. (1) and (2). Figure 3(b) also shows the momentum of $\gamma\gamma$ pairs for the $\pi^0\pi^0$ final state for events lying in region E of the $\mid \vec{p_{\mathrm{tot}}} \mid$ vs E_{tot} plot (Fig. 2) where the background at low energy is eliminated. The background below the peak was estimated by extrapolation of the spectrum at low momentum into the peak region. (See Fig. 3(a)). For the $\pi^0\pi^0$ channel the background was negligible $\ll 1\%$. Similar spectra were obtained for the $\pi^0\eta$ final state but in this case the number of events was corrected for a background contribution to the peak region of $\sim 8\%$.

The procedure for $\mathrm{K^0_L K^0_S}$ events with $\mathrm{K^0_S} \rightarrow \pi^0\pi^0$ and a non-interacting $\mathrm{K^0_L}$ was again similar but in this case the momentum distribution for the resulting 4γ was calculated. To make sure that the $\mathrm{K^0_L}$ was not lost in the hole around the beam pipe, events were selected with the measured momentum direction in the range $21^\circ < \theta < 159^\circ$ to ensure that the missing momentum of the non-interacting $\mathrm{K^0_L}$ points to a sensitive region of the calorimeter. The probability that a $\mathrm{K^0_L}$ of momentum $795\,\mathrm{MeV}/c$ does not interact in the crystals has previously been measured [10] to be $(43 \pm 3)\%$.

For the measurement of the $\pi^+\pi^-$ and $\mathrm{K^+K^-}$ branching ratios, 2-prong events recorded in the JDC were selected, requiring that the the number of 'hits' per track $\geq$ 15 with the track starting in layers 1-3 and finishing in layers 20-23. The momenta of the two-prong events were calculated and the distribution shows peaks close to $927.8\,\mathrm{MeV}/c$ due to $\pi^+\pi^-$ events and to $797.9\,\mathrm{MeV}/c$ due to $\mathrm{K^+K^-}$ pairs. Since the opening angle θ between the two tracks should be 180° it was further required that for the selected events $\cos(\theta) \leq -0.95$. For the plot of $\mid \vec{p_{\mathrm{tot}}} \mid$ as a function of E_{tot} it was assumed that all charged events

were pions. The fully reconstructed $\pi^+\pi^-$ final states then have total energy around $2m_{\rm p}c^2 = 1877\,\mathrm{MeV}$ whilst the $\mathrm{K^+K^-}$ final states apparently have a total energy of 1620 MeV as shown in figure 4. By choosing the selection region appropriately it is thus possible to distinguish between these two final states and to eliminate background. Plots of the momentum distribution of 2-prong events for the selected $\pi^+\pi^-$ and $\mathrm{K^+K^-}$ regions are shown in Figs. 5(a) and 5(b) respectively.

The detection efficiencies were calculated by Monte Carlo simulation using software based on the standard GEANT3.2 package. These simulated events were then passed through the same analysis chain as real data. The values for the finally selected energy/momentum regions for each channel are listed in Table 1 together with the corresponding number of data events. Corrections for the decay probability (0.3921) for $\eta \rightarrow 2\gamma$ and for the probability (0.3139) of $\mathrm{K^0_S} \rightarrow \pi^0\pi^0$ were applied using values from the Particle Data Group compilation [11]. After applying a factor of 0.963 to the total number of analysed events (1 591 407) to correct for annihilations outside the $\mathrm{H_2}$ target, the branching ratios listed in column 2 of Table 2 were obtained.

The data taken in July 1996 with a gaseous $\mathrm{H_2}$ target at room temperature and 12 bar pressure were analysed in a similar way. A total of 2 656 240 events were recorded and 2 593 580 remained after removal of events with the pile-up flag set. Of these 2 135 144 events contained charged tracks; their vertex z-distribution gave $\ll 1\%$ of annihilations occurring outside the target in the beam direction. Simulation calculations showed that between 2% and 5% of the incident antiprotons could stop in the target walls, the exact fraction depending on the antiproton beam parameters. The total number of analysed events was therefore corrected by a factor of 0.97 ± 0.02. The plots of momentum distributions and of $\mid \vec{p_{\rm tot}} \mid$ vs $E_{\rm tot}$ for both neutral and 2-prong events are very similar to those obtained with the liquid $\mathrm{H_2}$ target and are not repeated. The background correction to the number of $\pi^0\eta$ events $\sim 1\%$. The number of selected events and calculated detection efficiency are again given in Table 1. The reduced detection efficiency for the $\pi^+\pi^-$ and $\mathrm{K^+K^-}$ channels, compared to that obtained in liquid $\mathrm{H_2}$, is due to a slightly different alignment for the SVTX detector with respect to the JDC. The resulting measured branching ratios are listed in column 2 of Table 3.

3.2 All neutral data

As a further check on the reliability of the branching ratio measurements an analysis was made of a part of the "all neutral" data used in the previous Crystal Barrel publications [1,2], so as to obtain branching ratios for the $\pi^0\pi^0$ and $\pi^0\eta$ channels. This analysis was essentially a check of the earlier work but

using the updated and improved off-line analysis, reconstruction and kinematic fitting software now available. The analysis was also extended to the $\bar{p}p \to K^0_S K^0_L$ channel following the methods described in the previous Crystal Barrel measurement [10]. Detection efficiencies were again calculated using Monte Carlo simulated events. Corrections for in-flight annihilations $(5.7 \pm 1.1)\%$ and for antiprotons not stopping in the target $(3.9 \pm 0.7)\%$ were taken from the earlier work [2]. The results of this re-analysis of a part of the earlier "all neutral" data are given in Table 2 and are seen to be in good agreement with the previous results published by the Crystal Barrel collaboration [1,2,10] and with the results obtained using minimum bias data described above.

This analysis was repeated using the same methods but for data taken with the gaseous hydrogen target at 12 bar pressure. A total of $1.7\ 10^6$ events taken with an "all neutral" (AN) trigger were used to select $\pi^0\pi^0$, $\pi^0\eta$ and $K^0_S K^0_L$ events. The absolute normalisation used $\pi^0\pi^0$ events selected from $2.5\ 10^5$ "minimum bias" (MB) events taken during the same run period. After kinematic fitting to $\bar{p}p \to 4\gamma$ the branching ratios listed in column 3 of Table 3 were obtained using detector efficiencies calculated, as before, by Monte Carlo simulation. These are new measurements and are independent of those in column 2, described earlier, which were obtained with a minimum bias trigger.

4 Results

As we have previously remarked, the re-analysis of the liquid H_2 data gives results (Table 2) in good agreement with the earlier Crystal Barrel values [1,2,10]. The new analysis, which avoids biases due to kinematic fitting and uses data selection based solely on a $\mid \vec{p_{\rm tot}} \mid$ vs $E_{\rm tot}$ plot, likewise gives good agreement with the earlier work [1,2,10]. In particular it confirms a much larger value for the branching ratio $BR(\pi^0\pi^0, liq)$ than that measured recently by the Obelix collaboration [7] and most earlier experiments (See Ref.[12] for a more detailed discussion). We note that Crystal Barrel and Obelix are the only two experiments to measure all 4 photons and to fully reconstruct $\pi^0\pi^0$ events. The detection efficiency for $\pi^0\pi^0$ events is however much smaller for the Obelix experiment (0.062 ± 0.001), than for Crystal Barrel (0.637 ± 0.001), where the efficiency approaches the "geometrical" value of 0.662 for the detection of 4 photons. We note that the earlier measurement by the Obelix group [14] of the branching ratio in H_2 gas at density $\rho_{\rm STP}$ is also low when compared to the general trend of Crystal Barrel values as a function of target density plotted in Fig. 6(a).

The two measurements of the $\bar{p}p \to K^0_S K^0_L$ branching ratio in liquid H_2 (Table 2) with $K^0_S \to 2\pi^0$ are in good agreement with the value $BR(K^0_S K^0_L, liq) = (7.8 \pm 0.7 \pm 0.3)10^{-4}$ with $K^0_S \to \pi^+\pi^-$ measured by the Obelix collaboration

[13]. This good agreement is an important check on the consistency of the measurements from the two experiments, and particularly on the detection efficiency calculation for "all neutral" events in the Crystal Barrel detector.

The two values for $BR(\pi^0\pi^0, 12\,\rho_{\rm STP})$ measured in the present experiment (Table 3) are in good agreement. However the value for $BR(\mathrm{K^0_S K^0_L}, 12\,\rho_{\rm STP})$ obtained from the "minimum bias" analysis is significantly larger ($2.4\,\sigma$) than that obtained from the analysis of "all neutral" data. The latter value, however seems to be in general agreement with the overall trend of results for the $\mathrm{K^0_S K^0_L}$ branching ratio [10,13] when plotted as a function of target density ρ. (See Fig.6(b)). The reasons for this discrepancy are not understood. The value of the branching ratio obtained from the "minimum bias" data is stable against variation of the cuts in the $\mid \vec{p_{\rm tot}} \mid$ vs $E_{\rm tot}$ plot, suggesting that background events are not the cause of this apparently large value for the branching ratio.

Values for the $\pi^+\pi^-$ and $\mathrm{K^+K^-}$ branching ratios in liquid $\mathrm{H_2}$ (Table 2) are in good agreement with the previous Crystal Barrel measurements [2] and earlier work. (See Ref.[2] for a compilation of previous measurements.) The present measurements of $\pi^+\pi^-$ and $\mathrm{K^+K^-}$ branching ratios in $\mathrm{H_2}$ gas at $12\,\rho_{\rm STP}$ (Table 3) are in overall agreement with the trend of the branching ratio measurements as a function of target density shown in Figs. 6(c) and 6(d). In this figure the values of the branching ratios at $0.005\,\rho_{\rm STP}$ and $\rho_{\rm STP}$ are from the Obelix [15,16] and Asterix [3] experiments.

5 Fraction of P-state annihilation

The results reported here have been included in a new analysis of two-body branching ratios in terms of the fraction of P-state annihilation $\mathrm{f_P}(\rho)$, using the formalism described by Batty [5]. There it was shown that in the presence of Stark mixing it is necessary to take into account an enhancement of annihilation from fine structure states, over that expected from a purely statistical population of the levels. Fine structure widths predicted by various models are used, together with a cascade calculation, to calculate the "enhancement factors". This effect is particularly important for the $^3\mathrm{P_0}$ level, which has a very large width relative to the other P-states.

As well as the branching ratio data used in [5] and those from the present work, a number of recent measurements were also included. The Obelix collaboration [13] have measured branching ratios for the reaction $\mathrm{\bar{p}p \to K^0_S K^0_L}$; $\mathrm{K^0_S \to \pi^+\pi^-}$ at three densities, $0.005\,\rho_{\rm STP}$, $\rho_{\rm STP}$ and liquid, whilst the CPLEAR collaboration have measured [17] the ratio $BR(\mathrm{K^0_S K^0_S}, \rho)/BR(\mathrm{K^0_S K^0_L}, \rho)$ at densities of $15\,\rho_{\rm STP}$ and $27\,\rho_{\rm STP}$. This latter measurement enables the P-state fraction $\mathrm{f_P}(27\,\rho_{\rm STP})$ to be determined for the first time. Although not a two-body

branching ratio, the production of $\eta(1440)$ at three target densities in the reaction $\bar{\rm p}{\rm p}\to\eta(1440)\pi^+\pi^-$; $\eta(1440)\to {\rm K}^\pm{\rm K}^0_{\rm L}\pi^\mp$ has been determined [18] by the Obelix collaboration. This is a particularly useful measurement since the $\pi^+\pi^-$ dipion and the $\eta(1440)$ are produced with relative orbital angular momentum L = 0 and so production of the $\eta(1440)$ only occurs from the $^1{\rm S}_0$ state of the $\bar{\rm p}{\rm p}$ system [18] which does not contribute to the other two-body channels considered in this analysis. In bubble chamber data on $\bar{\rm p}{\rm p}\to\eta(1440)\pi^+\pi^-$; $\eta(1440)\to {\rm K}^\pm{\rm K}^0_{\rm S}\pi^\mp$ [19] however, a small contribution ($\approx 23\%$) due to annihilation from the $^3{\rm S}_1$ state was determined. In total we have 35 branching ratio measurements to be fitted by 17 parameters; 10 values of the partial branching ratios [5,12] $B(ch,{}^{2S+1}{\rm L}_J)$ and 7 values of the fraction of P-state annihilation ${\rm f_P}(\rho)$ over the range of target densities from $0.002\,\rho_{\rm STP}$ to liquid $\rm H_2$.

A least squares fit to the above data, but omitting the Obelix value [7] of $BR(\pi^0\pi^0,liq)$ which is much smaller than the measurements (Table 2) from the present experiment, gave a best fit with a χ^2 per degree of freedom $\chi^2/{\rm N} = 25.2/18$. Rather poorly fitted were the value of $BR({\rm K}^0_{\rm S}{\rm K}^0_{\rm L},12\,\rho_{\rm STP}) = (7.04\pm 0.74)10^{-3}$ measured in the present work with a minimum bias trigger (see column 2 of Table 3) and the value of $BR(\pi^0\pi^0,\rho_{\rm STP})$ measured by the Obelix experiment [14] which also gave difficulties in the previous analysis [5]. Values of χ^2 for these two measurements were 5.6 and 4.7 respectively. Omitting these two branching ratios gave a very good fit to the data with $\chi^2/{\rm N} = 13.7/16$. Calculated values of the branching ratios for this best fit solution are shown in Fig. 6, where for clarity the points have been joined by straight lines. Values obtained for the P-state fraction as a function of $\rm H_2$ target gas density ρ are given in Table 4. The reduction in the P-state fraction with increasing target density, due to the Stark effect, is clearly seen. These results were obtained with "enhancement factors" [5] calculated using the DR1 potential for the $\bar{\rm p}{\rm p}$ interaction [20]. The same values, within errors, were obtained using the DR2 and KW potentials [20]. A fit with the "enhancement factors" set to 1.0, i.e. neglecting fine structure effects, gave a significantly worse fit with $\chi^2/{\rm N} = 39.9/18$. For the DR1 "enhancement factors", including the Obelix value of $BR(\pi^0\pi^0,liq)$, but excluding the Crystal Barrel values, gave $\chi^2/{\rm N} = 27.2/17$ or $\chi^2/{\rm N} = 18.4/16$ when the value of $BR({\rm K}^0_{\rm S}{\rm K}^0_{\rm L},12\,\rho_{\rm STP}) = (7.04\pm 0.74)10^{-3}$ discussed above was omitted. In this fit the value obtained for the fraction of P-state annihilation in liquid $\rm H_2$ ${\rm f_P}(liq) = 0.06\pm 0.02$ whilst the values of ${\rm f_P}(\rho)$ at other pressures are the same within errors as those given in Table 4.

6 Summary

To summarise, values of the branching ratios for the reactions $\bar{\rm p}{\rm p}\to\pi^0\pi^0$, $\pi^0\eta$, ${\rm K}^0_{\rm L}{\rm K}^0_{\rm S}$, $\pi^+\pi^-$ and ${\rm K}^+{\rm K}^-$have been measured in liquid and gaseous ($12\,\rho_{\rm STP}$)

hydrogen. The results confirm the value of $BR(\pi^0\pi^0, liq)$ obtained previously by this collaboration [1] which is significantly larger than that obtained by the Obelix experiment [7]. The present branching ratio measurements have been compared with previous measured values (e.g. see Fig. 6). The results have been analysed, together with other data, using the formalism of Batty [5,12], to obtain the fraction of P-state annihilation at target densities from $0.002\,\rho_{\rm STP}$ to liquid H_2. The values, which are listed in Table 4, are similar to those obtained in the previous work [5] but are of improved accuracy and with additional values at 12 and $27\,\rho_{\rm STP}$.

Acknowledgement

We wish to thank A.Zoccoli and other members of the Obelix collaboration for very useful discussions regarding their branching ratio measurements. We would like to thank the technical staff of the LEAR machine group and of all the participating institutions for their invaluable contributions to the success of the experiment. We acknowledge financial support from the German Bundesministerium für Bildung, Wissenschaft, Forschung und Technologie, the Schweizerischer Nationalfonds, the British Particle Physics and Astronomy Research Council, the U.S. Department of Energy and the National Science Research Fund Committee of Hungary (contract No. DE-FG03-87ER40323, DE-AC03-76SF00098, DE-FG02-87ER40315 and OTKA T023635). K.M. Crowe and F.-H. Heinsius acknowledge support from the A. von Humboldt Foundation, and N. Djaoshvili from the DAAD.

References

[1] C. Amsler et al., Phys. Lett. B**297** (1992) 214.

[2] C. Amsler et al., Z. Phys. C**58** (1993) 175.

[3] M. Doser et al., Nucl. Phys. A**486** (1988) 493.

[4] J. M. Richard and M. E. Sanio, Phys. Lett. B**110** (1982) 349.

[5] C. J. Batty, Nucl. Phys. A**601** (1996) 425.

[6] C. J. Batty, Rep. Prog. Phys. **52** (1989) 1165.

[7] A. Zoccoli, Proceedings HADRON 97 conference (eds. S-U. Chung and H. J. Willutzki) AIP conference proceedings **432** (1998) 347.

[8] E. Aker et al., Nucl. Instr. Meth. Phys. Res. A **321** (1992) 69.

[9] M. Doser et al., Nucl. Instr. Meth. Phys. Res. A **412** (1998) 70.

[10] C. Amsler et al., Phys. Lett. B**346** (1995) 363.

[11] Particle Data Group, Eur. Phys. Jour. **3** (1998) 1.

[12] C. J. Batty, Nucl. Phys. A**655** (1999) 203c.

[13] A. Bertin et al., Phys. Lett. B**386** (1996) 486 and **389** (1996) 781.

[14] M. Agnello et al., Phys. Lett. B**337** (1994) 226.

[15] V. G. Ableev et al., Phys. Lett. B**329** (1994) 407.

[16] V. G. Ableev et al., Nuovo. Cim. **107A** (1994) 2837.

[17] R. Adler et al., Phys. Lett. B**403** (1997) 383.

[18] A. Bertin et al., Phys. Lett. B**385** (1996) 493 and **395** (1997) 388.

[19] P. Baillon et al., Nuovo. Cim. **50A** (1967) 393.

[20] J. Carbonell, G. Ihle and J. M. Richard, Z. Phys. A **334** (1989) 329.

[21] M. Doser et al., Phys. Lett. **B215** (1988) 792.

[22] C. Baltay et al., Phys. Rev. Lett. **15** (1965) 532.

Table 1
Number of selected events and detection efficiency for analysis with minimum bias data.

	Liquid H_2		$12\,\rho_{STP}$ H_2 gas	
Channel	Events	Detection efficiency	Events	Detection efficiency
$\pi^0\pi^0$	599	0.637 ± 0.032	2615	0.675 ± 0.034
$\pi^0\eta$	90	0.597 ± 0.030	353	0.636 ± 0.032
$K^0_S K^0_L$	88	0.495 ± 0.025	122	0.513 ± 0.026
$\pi^+\pi^-$	2417	0.479 ± 0.024	3859	0.379 ± 0.019
K^+K^-	737	0.439 ± 0.022	773	0.339 ± 0.017

Table 2
Branching ratios for $\bar{p}p$ annihilation in liquid H_2.

	Branching ratio in units 10^{-4}		
Channel	Min. Bias	Previous [2,10]	Re-analysis*
$\pi^0\pi^0$	6.14 ± 0.40	6.93 ± 0.43	7.17 ± 0.86
$\pi^0\eta$	2.50 ± 0.30	2.12 ± 0.12	1.98 ± 0.16
$K^0_S K^0_L$	8.64 ± 1.02	9.00 ± 0.60	8.75 ± 1.18
$\pi^+\pi^-$	33.0 ± 2.00	30.7 ± 1.30	
K^+K^-	11.0 ± 0.70	9.90 ± 0.50	

$\star$ only part of all neutral data used in [2,10].

Table 3
Branching ratios for $\bar{p}p$ annihilation in $12\,\rho_{STP}$ H_2 gas.

	Branching ratio in units 10^{-4}	
Channel	Min. Bias	AN. Trigger
$\pi^0\pi^0$	15.4 ± 0.88	16.2 ± 1.48
$\pi^0\eta$	5.63 ± 0.43	4.57 ± 0.30
$K^0_S K^0_L$	7.04 ± 0.74	4.89 ± 0.56
$\pi^+\pi^-$	40.5 ± 2.31	
K^+K^-	9.07 ± 0.59	

Table 4
Fraction of P-state annihilation as a function of H_2 target density.

Target density (units ρ_{STP})	P-state fraction
0.002	0.88±0.07
0.005	0.87±0.02
1.0	0.61±0.04
12.0	0.48±0.04
15.0	0.46±0.05
27.0	0.44±0.05
liq.	0.11±0.02

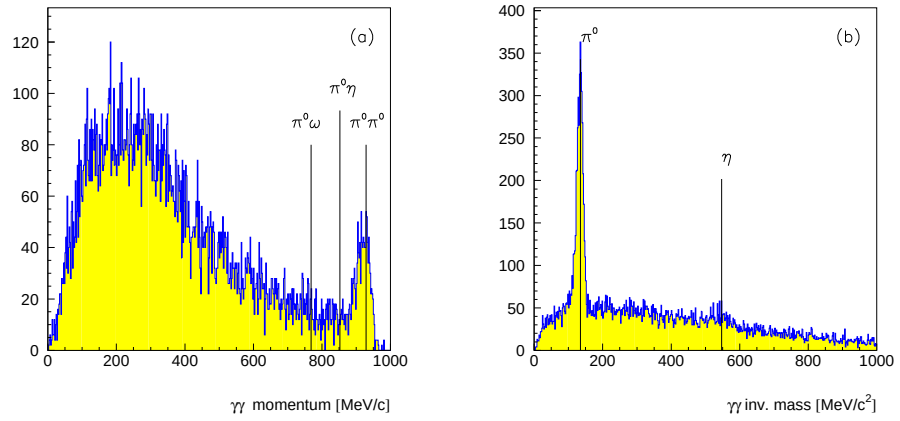

Fig. 1. Plots of (a) momentum and (b) invariant mass distributions for all six $\gamma\gamma$ combinations in the 4γ events selected from $\bar{p}p$ annihilations in liquid H_2.

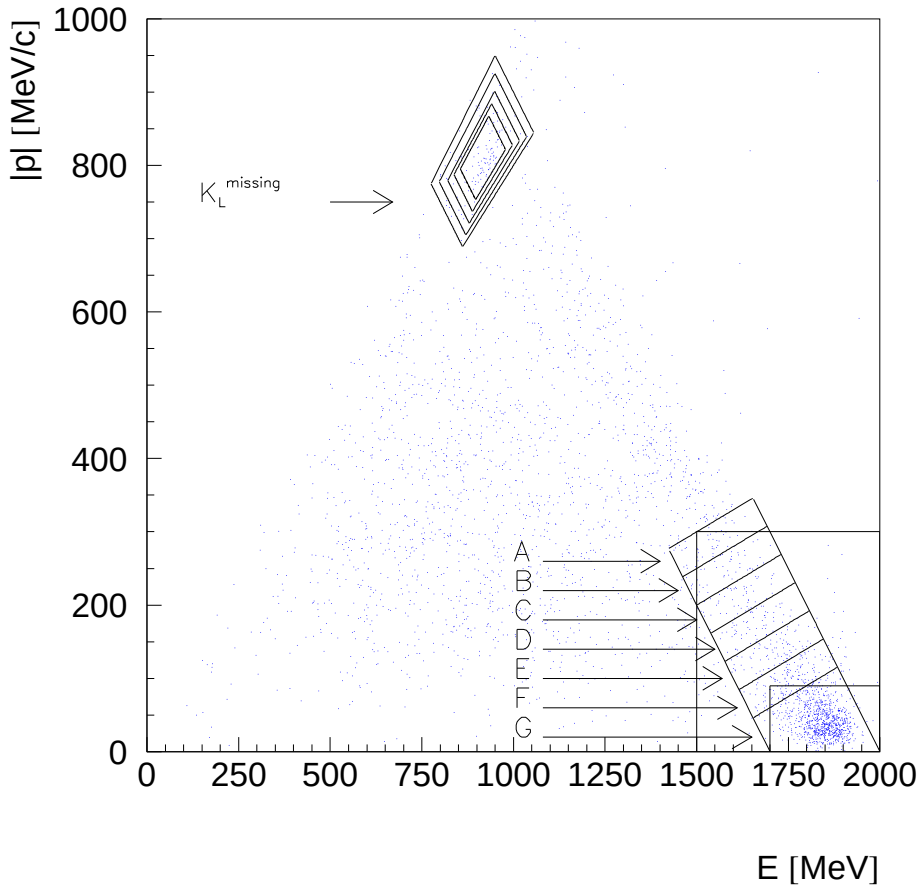

Fig. 2. Plot of total momentum $\mid \vec{p_{\rm tot}} \mid$ as a function of total energy $E_{\rm tot}$ for 4γ events selected from $\bar{\rm p}$p annihilations in liquid H_2. All of the selection regions labelled A to G extend to the $\mid \vec{p_{\rm tot}} \mid = 0$ axis.

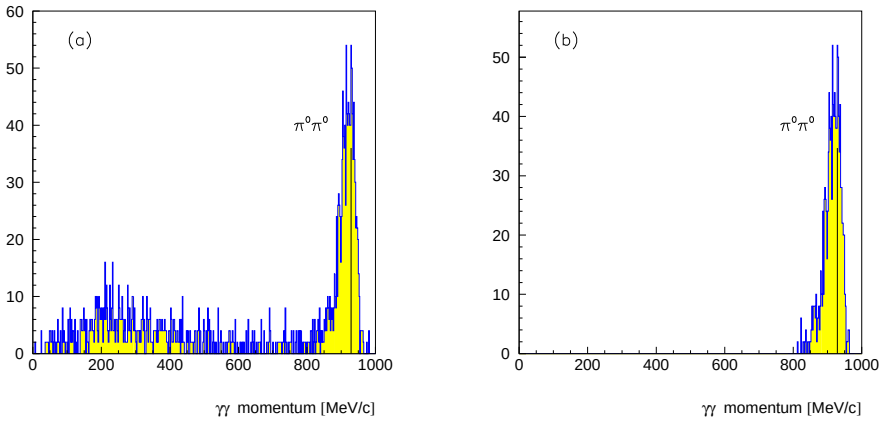

Fig. 3. Momentum distributions for (a) $\gamma\gamma$ pairs for the $\pi^0\pi^0$ final state which satisfy equs. (1) and (2); and (b) which also lie in the selected region E of the $\mid \vec{p_{\rm tot}} \mid$ vs $E_{\rm tot}$ plot shown in Figure 2.

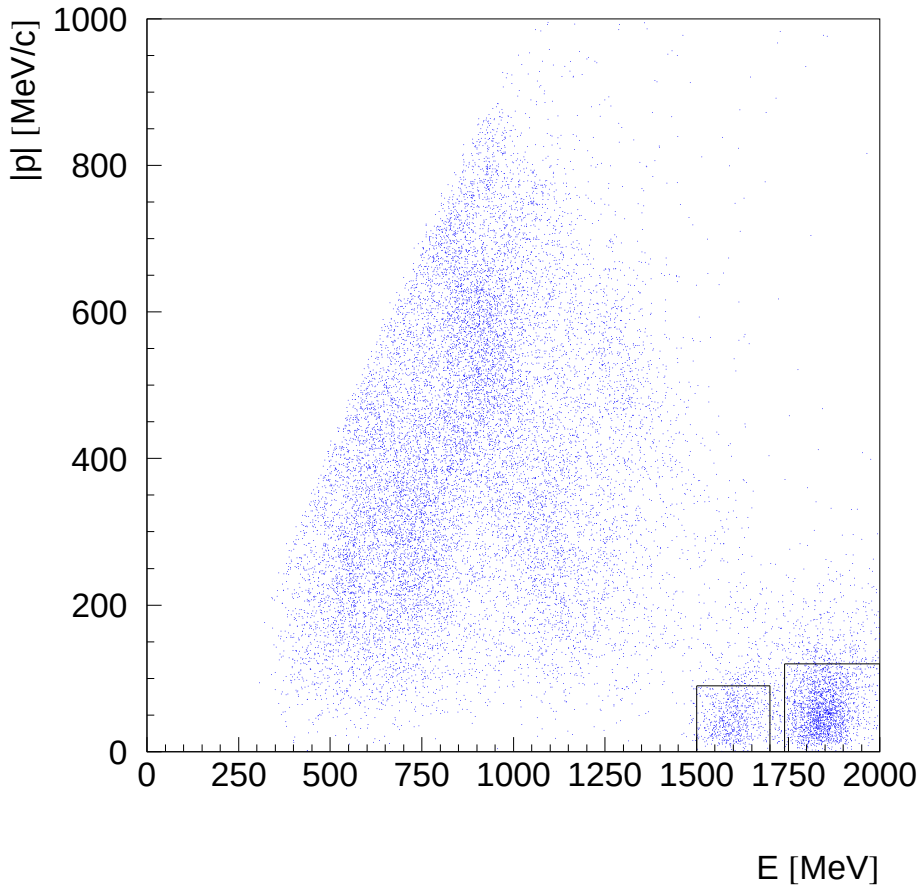

Fig. 4. Plot of total momentum $|\vec{p_{\rm tot}}|$ as a function of total energy $E_{\rm tot}$ for 2-prong events selected from $\bar{\rm p}$p annihilations in liquid H_2. The regions chosen for the final selection of K^+K^- (left) and $\pi^+\pi^-$ (right) events are shown.

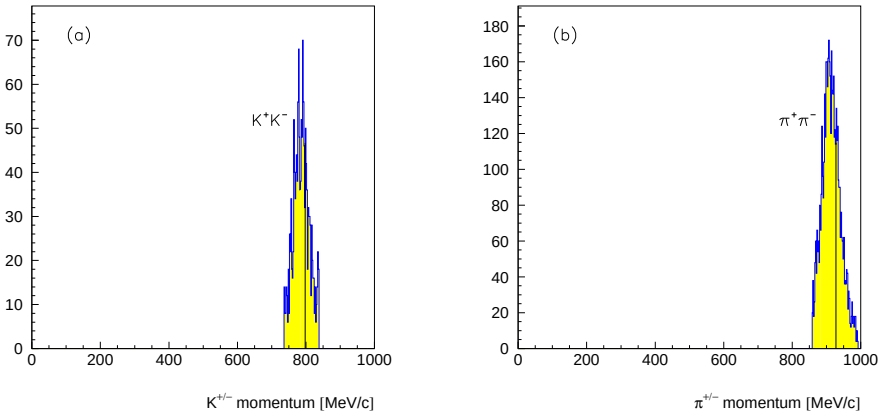

Fig. 5. Momentum distributions for the selected $\mid \vec{p_{\rm tot}} \mid$ vs $E_{\rm tot}$ plot regions for (a) K^+K^- and (b) $\pi^+\pi^-$ events from $\bar{\rm p}$p annihilations in liquid H_2. Values of (a) 798 MeV/c and (b) 928 MeV/c, as indicated by the vertical lines, are expected from 2-body kinematics.

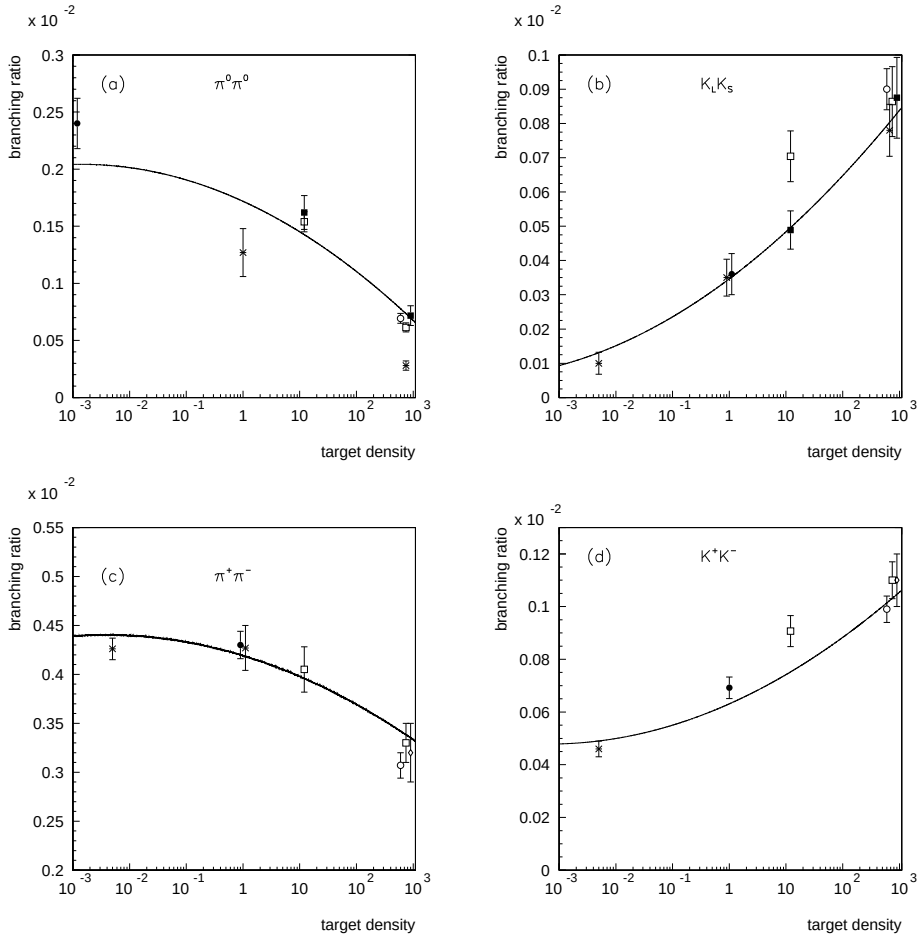

Fig. 6. Branching ratios for (a) $\bar{p}p \to \pi^0\pi^0$ (b) $\bar{p}p \to K^0_S K^0_L$ (c) $\bar{p}p \to \pi^+\pi^-$ (d) $\bar{p}p \to K^+K^-$ as a function of target density ρ (units ρ_{STP}). Values plotted are: ■ present work(Min.Bias), □ present work(A.N.Trigger), ○ Crystal Barrel [2] and (a) × Obelix [7,14], • Asterix [3]; (b) × Obelix [13], • Asterix [21]; (c) and (d) × Obelix [15,16], • Asterix [3], ◇ Bubble Chamber [22]. The curves are a smooth fit to branching ratios calculated from the fit to the data using the model of Batty [5].